NIH Public Access
Author Manuscript
Circulation. Author manuscript; available in PMC 2014 October 15.

Published in final edited form as:
Circulation. 2013 October 15; 128(16): 1758–1769. doi:10.1161/CIRCULATIONAHA.113.002885.

Impaired Cholesterol Metabolism and Enhanced Atherosclerosis in Clock Mutant Mice

Xiaoyue Pan, PhD, **Xian-Cheng Jiang, PhD**, and **M. Mahmood Hussain, PhD**
Departments of Cell Biology and Pediatrics, SUNY Downstate Medical Center, Brooklyn, NY

Abstract

Background—Clock is a key transcription factor that positively controls circadian regulation. However, its role in plasma cholesterol homeostasis and atherosclerosis has not been studied.

Methods and Results—We show for the first time that dominant-negative Clock mutant protein ($Clock^{\Delta 19/\Delta 19}$) enhances plasma cholesterol and atherosclerosis in three different mouse models. Detail analyses revealed that $Clk^{\Delta 19/\Delta 19}Apoe^{-/-}$ mice display hypercholesterolemia due to the accumulation of apoB48-containing cholesteryl ester-rich lipoproteins. Physiologic studies showed that enhanced cholesterol absorption by the intestine contributes to hypercholesterolemia. Molecular studies indicated that the expression of NPC1L1, ACAT2 and MTP in the intestines of $Clk^{\Delta 19/\Delta 19}Apoe^{-/-}$ mice was high and enterocytes assembled and secreted more chylomicrons. Further, we identified macrophage dysfunction as another potential cause of increased atherosclerosis in $Clk^{\Delta 19/\Delta 19}Apoe^{-/-}$ mice. Macrophages from $Clk^{\Delta 19/\Delta 19}Apoe^{-/-}$ mice expressed higher levels of scavenger receptors and took up more modified lipoproteins compared to $Apoe^{-/-}$ mice; but they expressed low levels of ABCA1 and were defective in cholesterol efflux. Molecular studies revealed that Clock regulates ABCA1 expression in macrophages by modulating USF2 expression.

Conclusions—$Clock^{\Delta 19/\Delta 19}$ protein enhances atherosclerosis by increasing intestinal cholesterol absorption, augmenting uptake of modified lipoproteins by macrophages, and reducing cholesterol efflux from macrophages. These studies establish that circadian Clock activity is crucial in maintaining low plasma cholesterol levels and in reducing atherogenesis in mice.

Keywords

Atherosclerosis; Circadian rhythm; Lipid metabolism; Cholesterol efflux; Clock; mouse Clock; ABCA1; USF2

Introduction

Circadian regulatory mechanisms synchronize biological functions to environmental stimuli such as light. Changes in light are transmitted from the eye by the retinal ganglion cells to

Correspondence: M. Mahmood Hussain, PhD Departments of Cell Biology and Pediatrics SUNY Downstate Medical Center 450 Clarkson Ave., Brooklyn, NY 11203 Phone: 718-270-4790 Fax: 718-270-2462 mahmood.hussain@downstate.edu.

Conflict of Interest Disclosures: None.

Disclaimer: The manuscript and its contents are confidential, intended for journal review purposes only, and not to be further disclosed.

This is a PDF file of an unedited manuscript that has been accepted for publication. As a service to our customers we are providing this early version of the manuscript. The manuscript will undergo copyediting, typesetting, and review of the resulting proof before it is published in its final citable form. Please note that during the production process errors may be discovered which could affect the content, and all legal disclaimers that apply to the journal pertain.

NIH-PA Author Manuscript
NIH-PA Author Manuscript
NIH-PA Author Manuscript

NIH-PA Author Manuscript

NIH-PA Author Manuscript

NIH-PA Author Manuscript

the suprachiasmatic nuclei in the brain where this information is translated into transcriptional regulation of certain transcription factors. Clock and Bmal1 are two transcription factors that increase expression of other transcription factors to control rhythmicity of different biological functions [1, 2]. Ablation of Clock has no significant effect on circadian rhythms as NPAS2 can substitute for Clock deficiency by interacting with Bmal1 [3, 4]. However, deletion of exon 19 in the *Clock* (*Clk*) gene results in the synthesis of $Clock^{\Delta 19/\Delta 19}$ mutant protein that acts as a dominant negative regulator and disrupts clock function [5, 6]. Mice expressing $Clock^{\Delta 19/\Delta 19}$ protein exhibit modest hypertriglyceridemia, hypercholesterolemia, hyperglycemia and hyperleptinemia [7]. We have previously shown that plasma triglyceride in $Clk^{\Delta 19/\Delta 19}$ mutant mice do not exhibit circadian rhythms, instead they show modest hypertriglyceridemia [8, 9]. Molecular studies showed that $Clock^{\Delta 19/\Delta 19}$ protein disrupts plasma triglyceride homoeostasis by deregulating diurnal transcriptional regulation of SHP and MTP [8]. In this study, we examined the effects of $Clock^{\Delta 19/\Delta 19}$ protein on the regulation of plasma cholesterol and atherosclerosis. Here, we show that $Clock^{\Delta 19/\Delta 19}$ protein enhances atherosclerosis and have identified different physiologic pathways and molecular targets affected by the expression of $Clock^{\Delta 19/\Delta 19}$ protein that contribute to atherosclerosis.

Methods

Animals

$Clk^{\Delta 19/wt}$, $Clk^{\Delta 19/wt}Ldlr^{-/-}$, and $Clk^{\Delta 19/wt}Apoe^{-/-}$ mice were bred to obtained $Clk^{\Delta 19/\Delta 19}$, $Clk^{wt/wt}$, $Clk^{\Delta 19/\Delta 19}Ldlr^{-/-}$, $Ldlr^{-/-}$, $Clk^{\Delta 19/\Delta 19}Apoe^{-/-}$ and $Apoe^{-/-}$ mice. All mice on C57/Bl6 background were housed with a 12-hour lighting schedule (700–1900 hours). Male, 2-3 months old mice were fed different diets (Table S1) for atherosclerosis studies. Animal experiments were approved by the Animal Care and Use Committee of the SUNY Downstate Medical Center and were performed in accordance with institutional guidelines.

Macrophages

Bone marrow-derived macrophages obtained from $Clk^{\Delta 19/\Delta 19}Apoe^{-/-}$ mice and $Apoe^{-/-}$ mice [10] were treated with or without oxLDL for 8 hours. For cholesterol efflux assays, macrophages were labeled with [^{3}H]cholesterol for 24 h, washed with PBS, incubated in DMEM containing 0.2% BSA for 1 h and then in the same media in the absence or presence of apoAI (15 μg/ml) or HDL (50 μg/ml) for 8 hours. The human monocytic cell line THP-1 was maintained in RPMI 1640 media and differentiated by treating with phorbol myristic acid.

Plasma lipids

After 4-h fast, plasma was obtained to measure lipids using kits. Plasma apoA-I, apoB and apoE were quantified by western blotting [11]. Mice were not fasted when daily changes in plasma and tissue lipids were studied.

In vivo absorption of lipids

Mice were injected intraperitoneally with 0.5 ml of Poloxamer P407 in PBS (1:6, v/v) and gavaged with [^{3}H]cholesterol at 12:00.

Uptake and secretion of lipids by enterocytes

To study uptake, enterocytes from $Clk^{\Delta 19/\Delta 19}Apoe^{-/-}$ mice and $Apoe^{-/-}$ mice were incubated in triplicate with [^{3}H]cholesterol (1 μCi/ml) for different times. To measure secretion, enterocytes were incubated in triplicate with [^{3}H]cholesterol for 1 h, washed and then incubated in fresh media containing oleic acid and taurocholate for different time [12]. To

NIH-PA Author Manuscript

NIH-PA Author Manuscript

NIH-PA Author Manuscript

study the distribution of cholesterol in chylomicrons and HDL, conditioned media was adjusted to a density of 1.10 g/ml by the addition of KBr and overlaid with different density solution and centrifuged [12].

Evaluation of atherosclerosis

The proximal aorta was collected after saline perfusion. The aortic root and ascending aorta were sectioned at a thickness of 10 μm, and alternate sections were saved on slides for staining [13].

In vivo macrophage cholesterol efflux measurement [10, 14]

J774A.1 cells were grown in suspension in DMEM medium supplemented with 10% fetal bovine serum. Cells were radiolabeled with 5 μCi/mL ^{3}H-cholesterol and 50 μg/mL acetylated LDL for 48 hours. The labeled foam cells were injected intraperitoneally into $Clk^{\Delta 19/\Delta 19}Apoe^{-/-}$ and $Apoe^{-/-}$ mice. Blood, feces and liver were collected for counting. Bone marrow-derived macrophages derived from $Clock^{\Delta 19/\Delta 19}Apoe^{-/-}$ mice and $Apoe^{-/-}$ mice were incubated with acetylated LDL and [^{3}H]cholesterol, and injected into WT mice.

Chromatin immunoprecipitation (ChIP) assay

ChIP was used to study the binding of different transcription factors to the *ABCA1* promoter using goat polyclonal antibodies against HIF1α, HIF1β, USF1, and USF2 using kits as reported [8]. ABCA1 promoter sequences were amplified using primers (Table S2).

Bone marrow transplantation

$Apoe^{-/-}$ mice (age 8 weeks) were lethally irradiated and transplanted with bone marrow cells derived from $Clk^{\Delta 19/\Delta 19}Apoe^{-/-}$ or $Apoe^{-/-}$ mice.

Statistical analyses

Data are presented as mean ± SD, n=6-12 animals. Mice were sacrificed at each time point and plasma and tissue samples were collected. Statistical testing was performed by the paired Student's *t*-test. Temporal comparisons between two groups were performed using two-way ANOVA followed by Boneferroni post-test (GraphPad Prism). Differences were considered statistically significant when $P < 0.05$.

Results

$Clk^{\Delta 19/\Delta 19}$ mice develop atherosclerosis on an atherogenic diet

To test the hypothesis that $Clk^{\Delta 19/\Delta 19}$ mice might be susceptible to atherosclerosis, wildtype (WT, $Clk^{wt/wt}$) and $Clk^{\Delta 19/\Delta 19}$ siblings were fed either chow or an atherogenic diet [15] *ad libitum*. Chow fed $Clk^{\Delta 19/\Delta 19}$ mice had higher lipids compared to their WT siblings (Table 1) but did not show any atherosclerotic lesions. However, after feeding an atherogenic diet for 2 months, $Clk^{\Delta 19/\Delta 19}$ mice had 2- to 3-fold higher plasma cholesterol and triglyceride (Table 1) mainly in VLDL/IDL/LDL (Fig S1A-B), increased amounts of ApoB100 and ApoB48 but reduced levels of ApoA1 and ApoE (Fig S1C), and higher ApoB/ApoAI ratios (Fig S1D) compared to WT siblings. These mice had 2.3- and 1.6- fold more lesions at the aortic arches (Fig 1A) and aortic root (Fig 1B), respectively, and 3- to 4-fold elevated amounts of lipid lesions in the abdominal aorta (Fig 1C). Thus, $Clk^{\Delta 19/\Delta 19}$ mice show hyperlipidemia and develop more lesions on an atherogenic diet.

NIH-PA Author Manuscript
NIH-PA Author Manuscript
NIH-PA Author Manuscript

Clock mutant protein increases atherosclerosis in *Ldlr*$^{-/-}$ mice

Besides feeding an atherogenic diet, atherosclerosis is commonly studied in mouse models deficient in LDL receptors and ApoE [16]. *Clk*$^{\Delta 19/\Delta 19}$*Ldlr*$^{-/-}$ mice had higher plasma lipids when fed chow and western diets (Table 1) and developed more atherosclerotic lesions than *Ldlr*$^{-/-}$ mice both on chow and western diets, respectively (Fig 1D-F).

Clock mutant protein increases atherosclerosis in chow fed *Apoe*$^{-/-}$ mice

Next, we studied the effect of Clock$^{\Delta 19/\Delta 19}$ protein on atherosclerosis in *Apoe*$^{-/-}$ mice. *Clk*$^{\Delta 19/\Delta 19}$*Apoe*$^{-/-}$ mice on chow diet showed more extensive atherosclerotic lesions in the aortic arch than *Apoe*$^{-/-}$ mice (Fig 2A). The whole aorta showed 34-fold increased lipid staining (Fig 2B) whereas cardiac/aortic junctions of *Clk*$^{\Delta 19/\Delta 19}$*Apoe*$^{-/-}$ mice had 22-fold more lipid lesions. The lesions at the cardiac/aortic junction contained 4-fold higher necrotic core (Fig 2C) and macrophages (Fig 2D). Further, smooth muscle cells (Fig 2E) and collagen content (Fig 2F) were increased by 5-fold. These observations indicate for the presence of advanced, stable plaques in *Clk*$^{\Delta 19/\Delta 19}$*Apoe*$^{-/-}$ mice. These lesions were more in male than in female mice and their size increased with age (Fig S2). Brachiocephalic artery (BCA) of these mice had higher amounts of cholesterol/cholesteryl esters/triglycerides (Fig S3A), lipids (Fig S3B), necrotic area (Fig S3C), macrophages (Fig S3D), smooth muscle cells (Fig S3E) and collagen (Fig S3F). *Clk*$^{\Delta 19/\Delta 19}$*Apoe*$^{-/-}$ mice developed more atherosclerotic lesions on a western diet (Fig S4). These studies indicate that *Clk*$^{\Delta 19/\Delta 19}$*Apoe*$^{-/-}$ mice develop extensive lesions throughout the aorta that are rich in lipids, macrophages, smooth muscle cells and collagen compared to *Apoe*$^{-/-}$ mice, most likely representing stable plaques.

Plasma lipids are higher in *Clk*$^{\Delta 19/\Delta 19}$Apoe$^{-/-}$ mice

Plasma of chow fed *Clk*$^{\Delta 19/\Delta 19}$*Apoe*$^{-/-}$ mice was more turbid (Fig 3A) and had 2-fold higher amounts of total and esterified cholesterol (Table 1). Plasma total cholesterol levels were significantly higher and triglyceride levels were lower in these mice at all time points (Fig S5). Cholesterol levels were higher in non-HDL lipoproteins but were lower in HDL (Table 1). Plasma ApoB100 and ApoAI levels were lower (Fig 3C, protein blot); but ApoB48 and ApoB/ApoAI ratios were higher in these mice (Fig 3C). These studies indicate that *Clk*$^{\Delta 19/\Delta 19}$*Apoe*$^{-/-}$ mice accumulate more ApoB48-containing cholesteryl ester-rich lipoproteins.

Clk$^{\Delta 19/\Delta 19}$Apoe$^{-/-}$ mice absorb more cholesterol

Since lipoprotein catabolism is impaired in *Apoe*$^{-/-}$ mice, we hypothesized that higher plasma ApoB48-containing cholesteryl ester-rich lipoproteins are due to increased cholesterol absorption by the intestine. To study absorption, mice were gavaged with radiolabeled cholesterol. Radiolabeled cholesterol derived lipids were higher at 2-4 h in the plasma of *Clk*$^{\Delta 19/\Delta 19}$*Apoe*$^{-/-}$ mice (Fig 3D). Increased absorption could be due to increased uptake and/or secretion by enterocytes. Isolated primary enterocytes from *Clk*$^{\Delta 19/\Delta 19}$*Apoe*$^{-/-}$ mice took up more cholesterol in a time-dependent manner (Fig 3E). Further, pulse-chase studies showed that enterocytes secrete more cholesterol (Fig 3F). These studies revealed that uptake and secretion of cholesterol are higher in *Clk*$^{\Delta 19/\Delta 19}$*Apoe*$^{-/-}$ enterocytes.

Cholesterol uptake in enterocytes is a balance between import by NPC1L1 and export by ABCG5/ABCG8 [17]. Measurement of mRNA levels revealed no change in ABCG5/ABCG8 (Fig 3G); instead we found significant increases in NPC1L1 mRNA (Fig 3G) and protein (Fig 3H) levels. Therefore, increased expression of NPC1L1 might contribute to increased uptake of cholesterol in *Clk*$^{\Delta 19/\Delta 19}$*Apoe*$^{-/-}$ enterocytes.

NIH-PA Author Manuscript

NIH-PA Author Manuscript

NIH-PA Author Manuscript

After uptake, cholesterol is secreted by enterocytes via HDL and chylomicrons [18]. HDL pathway transports free cholesterol involving ABCA1 and ApoAI. We found that ABCA1 was reduced but ApoA1 mRNA were similar in the enterocytes of *Clk*$^{\Delta 19/\Delta 19}$*Apoe*$^{-/-}$ and in *Apoe*$^{-/-}$ mice (Fig 3G). The transport of cholesterol via chylomicrons depends on ACAT enzymes and MTP, as dietary cholesterol is esterified by ACAT1/ACAT2, packaged in chylomicrons by MTP and secreted. We observed significant increases in ACAT2, but not ACAT1, mRNA levels in *Clk*$^{\Delta 19/\Delta 19}$*Apoe*$^{-/-}$ mice (Fig 3G). Moreover, MTP protein, mRNA (Fig 3G-H), and activity (Fig 3I) were significantly higher in *Clk*$^{\Delta 19/\Delta 19}$*Apoe*$^{-/-}$ mice. Increases in MTP and ACAT2 suggested that chylomicron assembly and secretion pathway might be augmented in *Clk*$^{\Delta 19/\Delta 19}$*Apoe*$^{-/-}$ mice. To test this, we incubated enterocytes with radiolabeled cholesterol and conditioned media was subjected to ultracentrifugation. Cholesterol counts were higher in chylomicrons but not in HDL fractions (Fig 3J) indicating that *Clk*$^{\Delta 19/\Delta 19}$*Apoe*$^{-/-}$ mice absorb more cholesterol by enhancing assembly and secretion of chylomicrons.

Plasma cytokines are higher in Clk$^{\Delta 19/\Delta 19}$Apoe$^{-/-}$ mice

Inflammation is a hallmark of atherosclerosis. Therefore, we measured cytokines in *Clk*$^{\Delta 19/\Delta 19}$*Apoe*$^{-/-}$ and *Apoe*$^{-/-}$ mice. Plasma of *Clk*$^{\Delta 19/\Delta 19}$*Apoe*$^{-/-}$ mice contained ~2- to 4-fold higher levels of IL12, IL17A and G-CSF (Fig S6A). It is known that macrophages contribute to plasma cytokines. Therefore, we looked at the expression of several of these cytokines in bone marrow derived macrophages. *Clk*$^{\Delta 19/\Delta 19}$*Apoe*$^{-/-}$ macrophages had higher mRNA levels of IL12, IL6, TNFα and G-CSF but not IL17A (Fig S6B); IL17 is mainly produced by lymphocytes [19]. To determine whether Clock plays a role in the regulation of cytokine expression, we reduced Clock levels using siRNA in WT macrophages. siClock reduced Clock mRNA by 80% (Fig S5C) and increased G-CSF and GM-CSF. These studies suggest that Clock suppresses expression of different cytokines in macrophages.

Clk$^{\Delta 19/\Delta 19}$Apoe$^{-/-}$ macrophages take up more modified lipoproteins due to increased expression of CD36 and SR-A1

Studies described above showed that lesions in *Clk*$^{\Delta 19/\Delta 19}$*Apoe*$^{-/-}$ mice were lipid and macrophage rich (Figs 2B, 2D, S3B, S3D). To understand mechanisms that might contribute to accumulation of lipids in the aorta, we injected DiI-labeled AcLDL into *Apoe*$^{-/-}$ and *Clk*$^{\Delta 19/\Delta 19}$*Apoe*$^{-/-}$ mice. There was 2-fold higher DiI-label in the aorta of *Clk*$^{\Delta 19/\Delta 19}$*Apoe*$^{-/-}$ mice than *Apoe*$^{-/-}$ mice (Fig 4A). It is known that macrophages are the principal cells that take up modified lipoproteins in the subintima; therefore, we studied the uptake of modified lipoproteins by bone marrow derived macrophages from *Clk*$^{\Delta 19/\Delta 19}$*Apoe*$^{-/-}$ and *Apoe*$^{-/-}$ mice. Compared with *Apoe*$^{-/-}$ mice, *Clk*$^{\Delta 19/\Delta 19}$*Apoe*$^{-/-}$ macrophages took up 2-fold higher amounts of DiI-labeled Ac-LDL, contained 2- to 3-fold higher amounts of lipids, lipid peroxides, as well as total and esterified cholesterol (Fig 4B-E). To explore reasons for lipid accumulation, we measured mRNA and protein levels of scavenger receptors involved in the uptake of modified lipoproteins. *Clk*$^{\Delta 19/\Delta 19}$*Apoe*$^{-/-}$ macrophages expressed higher protein and mRNA levels of CD36 and SR-A1 (Fig 4F) suggesting that their increased expression could contribute to fat accumulation.

Clk$^{\Delta 19/\Delta 19}$ reduces Clock activity by acting as a dominant negative mutant [5]. Therefore, to understand mechanisms for increased expression of scavenger receptors, we reduced Clock expression using siRNA in *Clk*$^{wt/wt}$ macrophages. siClock reduced Clock mRNA levels by ~80% in wildtype macrophages and these levels were unaffected by oxLDL treatment (Fig 4G). Reductions in Clock had no effect on the mRNA (Fig 4G) and protein (Fig 4H) levels of CD36 and SR-A1 in normal macrophages. However, incubation of these macrophages with ox-LDL increased expression of scavenger receptors in both siControl and siClock treated cells; but, increases in the protein and mRNA levels of these scavenger receptors

NIH-PA Author Manuscript

NIH-PA Author Manuscript

NIH-PA Author Manuscript

were higher in siClock treated cells (Fig 4G-H). Further, siClock treated macrophages took up 2-fold higher amounts of DiI-labeled AcLDL (Fig 4I). Similarly, siClock treated human THP-1 macrophages took up more DiI-AcLDL (Fig S7A). These studies show that increases in scavenger receptors were higher when macrophages have reduced Clock expression and are exposed to ox-LDL. Thus, Clock reduces expression of scavenger receptors when macrophages are exposed to modified lipoproteins.

Clk$^{\Delta 19/\Delta 19}$Apoe$^{-/-}$ macrophages are defective in cholesterol efflux due to reduced ABCA1 expression

Apart from increased uptake, reduced efflux also contributes to cholesterol accumulation in macrophages. Therefore, we studied *in vivo* reverse cholesterol transport from ^{3}H-cholesterol loaded J774 macrophages in *Apoe*$^{-/-}$ and *Clk*$^{\Delta 19/\Delta 19}$*Apoe*$^{-/-}$ mice. Appearance of cholesterol into plasma, feces and liver was significantly less in *Clk*$^{\Delta 19/\Delta 19}$*Apoe*$^{-/-}$ mice compared to *Apoe*$^{-/-}$ mice (Fig 5A) indicating that *Clk*$^{\Delta 19/\Delta 19}$*Apoe*$^{-/-}$ plasma is less efficient in reverse cholesterol transport from J774 macrophages most likely secondary to low plasma HDL (Table 1) and ApoAI (Fig 3C) in these mice. Additionally, we studied the ability of *Clk*$^{\Delta 19/\Delta 19}$*Apoe*$^{-/-}$ macrophages to give up cholesterol to plasma acceptors in WT mice. Injection of ^{3}H-cholesterol loaded *Clk*$^{\Delta 19/\Delta 19}$*Apoe*$^{-/-}$ or *Apoe*$^{-/-}$ macrophages into WT mice revealed that *Clk*$^{\Delta 19/\Delta 19}$*Apoe*$^{-/-}$ macrophages are defective in giving off cholesterol as evidenced by lower amounts of cholesterol in plasma, feces and liver (Fig 5B). Further, isolated *Clk*$^{\Delta 19/\Delta 19}$*Apoe*$^{-/-}$ macrophages gave up less cholesterol to extracellular ApoAI and HDL in culture (Fig 5C). Thus, *Clk*$^{\Delta 19/\Delta 19}$*Apoe*$^{-/-}$ macrophages are defective in cholesterol efflux.

Clock regulates ABCA1 expression

To understand reasons for reduced cholesterol efflux, we measured mRNA and protein levels of transporters involved in cholesterol efflux and found lower amounts of ABCA1 and ABCG1 mRNA and protein levels in *Clk*$^{\Delta 19/\Delta 19}$*Apoe*$^{-/-}$ macrophages, but no change in SR-B1 and ABCG4 expression (Fig 5D). To determine whether low expression of ABCA1 was contributing to reduced cholesterol efflux, we expressed ABCA1 under the control of cytomegalovirus promoter. Over expression of ABCA1 increased cholesterol efflux from *Clk*$^{\Delta 19/\Delta 19}$*Apoe*$^{-/-}$ macrophages (Fig 5E).Next, we asked whether Clock regulates ABCA1. First, we asked whether ApoE deficiency is required for Clock$^{\Delta 19/\Delta 19}$ to reduce ABCA1. This was not the case as ABCA1 levels were low in *Clk*$^{\Delta 19/\Delta 19}$ macrophages compared to their WT littermates (Fig 5F). Second, knockdown of Clock in *Clk*$^{wt/wt}$ macrophages reduced ABCA1 mRNA (Fig 5G) and protein (Fig 5H, inset) levels as well as efflux to ApoAI (Fig 5H). Similarly, Clock knockdown in human THP-1 macrophages reduced cholesterol efflux to HDL and apoAI (Fig S7B-C). In contrast, knockdown of PER1, CRY1 or BMAL1 in *Clk*$^{wt/wt}$ macrophages had no effect on ABCA1 mRNA (Fig S8A) and cholesterol efflux (Fig S8B). These data suggest that Clock regulates ABCA1 expression and cholesterol efflux.

Clock modulates ABCA1 expression involving USF2

To determine whether Clock regulates ABCA1 at the transcriptional level, we expressed luciferase under the control of 1.3 kb ABCA1 promoter [20] along with a Clock expression plasmid or lentiviruses expressing shClock in wildtype macrophages. Over expression of Clock increased while its knockdown significantly reduced promoter activity (Fig 6A) suggesting that Clock increases ABCA1 transcription. To identify transcription factors regulated by Clock and those involved in ABCA1 expression, we measured mRNA levels of various activators and repressors that are known to regulate ABCA1 gene expression [21]. Activators of ABCA1 were either reduced or did not change in *Clk*$^{\Delta 19/\Delta 19}$*Apoe*$^{-/-}$

NIH-PA Author Manuscript

NIH-PA Author Manuscript

NIH-PA Author Manuscript

macrophages compared to *Apoe*$^{-/-}$ macrophages (Fig S9A). Quantifications of various repressors showed that USF1, USF2 and TRβ were significantly increased (Fig S9B). Further, knockdown of Clock in WT macrophages either reduced or had no effect on activators (Fig S9C). Although siClock had no significant effect on various repressors, it significantly increased mRNA (Fig S9D) and protein (Fig 6B) levels of USF1 and USF2. These studies suggested that Clock may modulate USF1 and USF2 expression to regulate ABCA1.

Subsequently, we determined the role of USF1 and USF2 in the regulation of ABCA1 by Clock. USF1/USF2 and HIF1α/HIF1β bind to an E-box in the ABCA1 promoter to decrease and increase ABCA1 expression, respectively [21, 22]. Knockdown of USF1, USF2, HIF1α and HIF1β had no effect on Clock mRNA suggesting that Clock is not regulated by them (Fig S10). siUSF1 and siUSF2 increased ABCA1 expression but siHIF1α and siHIF1β had no effect (Fig 6C) pointing out that USF1 and USF2 suppress ABCA1 expression. Therefore, we asked whether Clock needs these transcription factors to regulate ABCA1. siClock reduced ABCA1 expression in siHIF1α, siHIF1β and siUSF1 treated cells but not in siUSF2 treated cells (Fig 6C) indicating that siClock needs USF2 to reduce ABCA1 expression. To confirm the role of USF2 in ABCA1 regulation, we performed ChIP in *Apoe*$^{-/-}$ and *Clk*$^{\Delta 19/\Delta 19}$*Apoe*$^{-/-}$ macrophages. In *Apoe*$^{-/-}$ macrophages, ABCA1 promoter was occupied by Hif1β, USF1 and USF2 (Fig 6D). However, in *Clk*$^{\Delta 19/\Delta 19}$*Apoe*$^{-/-}$ macrophages only USF1 and USF2 were found associated with the promoter. The amounts of USF2 associated with the promoter were higher in *Clk*$^{\Delta 19/\Delta 19}$*Apoe*$^{-/-}$ macrophages. Therefore, increased binding of USF2 to the ABCA1 promoter in *Clk*$^{\Delta 19/\Delta 19}$*Apoe*$^{-/-}$ macrophages might reduce expression.

To garner *in vivo* significance of USF2 in cholesterol efflux, we hypothesized that reduction of USF2 in *Clk*$^{\Delta 19/\Delta 19}$*Apoe*$^{-/-}$ macrophages might enhance reverse cholesterol transport. To test this, bone marrow derived *Clk*$^{\Delta 19/\Delta 19}$*Apoe*$^{-/-}$ macrophages were treated with siControl or siUSF2, loaded with ^{3}H-cholesterol and injected in wildtype mice. After 48 h, mice receiving siUSF2 treated macrophages contained higher ^{3}H-cholesterol levels in the plasma, liver and feces (Fig 6E). These studies indicate that siUSF2 increases reverse cholesterol transport from macrophages.

Cyclic expression of ABCA1 and USF2 in macrophages

The above studies indicated that Clock regulates macrophage ABCA1 expression and cholesterol efflux by regulating USF2. Nothing is known about the circadian regulation of ABCA1 and USF2 in macrophages or in other cells. To determine whether ABCA1 and USF2 expression shows diurnal changes, WT bone marrow macrophage cultures treated or not with siClock were synchronized by incubating them in 50% serum for 2 h. Subsequently, changes in macrophage ABCA1 and USF2 were measured at different times. ABCA1 and USF2 expression showed cyclic expression in synchronized WT macrophages. ABCA1 and USF2 levels increased and decreased, respectively, in siClock treated macrophages (Fig 6F). Further, ABCA1 mRNA levels were low when USF2 levels were high. These studies indicate that ABCA1 and USF2 expression in macrophages shows cyclic change and Clock plays an important role in these changes.

Effect of *Clk*$^{\Delta 19/\Delta 19}$Apoe$^{-/-}$ bone marrow cell transplantation on atherosclerosis in *Apoe*$^{-/-}$ mice

To determine whether macrophage dysfunction contributes to increased atherosclerosis independent of hyperlipidemia, we transplanted bone marrow cells obtained from *Clk*$^{\Delta 19/\Delta 19}$*Apoe*$^{-/-}$ or *Apoe*$^{-/-}$ mice into lethally irradiated *Apoe*$^{-/-}$ mice. Bone marrow transplantation slightly reduced total plasma cholesterol in *Apoe*$^{-/-}$ mice (Fig 7A). However,

NIH-PA Author Manuscript

NIH-PA Author Manuscript

NIH-PA Author Manuscript

Apoe$^{-/-}$ mice that received bone marrow cells from *Clk*$^{\Delta 19/\Delta 19}$*Apoe*$^{-/-}$ mice had 2- to 2.7-fold higher atherosclerotic plaques in the ascending aortas and three main branching arteries (Fig 7B) and at the cardiac/aortic junctions (Fig 7C). Further, there was 3-fold higher lipid staining in the aorta (Fig 7D). Moreover, macrophages obtained from mice transplanted with bone marrow cells from *Clk*$^{\Delta 19/\Delta 19}$*Apoe*$^{-/-}$ were defective in cholesterol efflux to ApoAI and HDL (Fig 7E). Gene expression analysis showed that macrophages isolated from *Apoe*$^{-/-}$ mice transplanted with *Clk*$^{\Delta 19/\Delta 19}$*Apoe*$^{-/-}$ bone marrow cells had low mRNA levels of ABCA1/ABCG1 and higher levels of CD36/SR-A1 (Fig 7F). Further analysis of transcription factors that regulate ABCA1 revealed that these macrophages had higher levels of USF2 (Fig 7G). Thus, macrophage dysfunction due to the expression of Clock$^{\Delta 19/\Delta 19}$ protein contributes to atherosclerosis in *Apoe*$^{-/-}$ mice.

Discussion

Using three different mouse models and three different diets we show for the first time that Clock dysfunction due to the expression of a dominant negative Clock$^{\Delta 19/\Delta 19}$ protein increases atherosclerosis in mice. Different mouse models carrying Clock$^{\Delta 19/\Delta 19}$ protein had higher cholesterol in apoB-containing non-HDL lipoproteins. Mechanistic studies revealed that Clock$^{\Delta 19/\Delta 19}$ protein enhances cholesterol absorption by enterocytes and uptake of modified lipoproteins by macrophages in *Apoe*$^{-/-}$ mice. In contrast, it reduces cholesterol efflux from macrophages. Thus, Clock plays an important and novel role in the regulation cholesterol metabolism in enterocytes and macrophages to prevent hypercholesterolemia and atherosclerosis. Biochemical analysis showed that hypercholesterolemia in *Clk*$^{\Delta 19/\Delta 19}$*Apoe*$^{-/-}$ mice was due to accumulation of cholesteryl ester-rich ApoB48-containing lipoproteins. Physiologic studies showed that enterocytes expressing Clock$^{\Delta 19/\Delta 19}$ protein take up more cholesterol from the intestinal lumen and secrete more cholesterol with chylomicrons. Molecular studies demonstrated that increased cholesterol uptake was associated with enhanced expression of NPC1L1with no significant changes in cholesterol exporters ABCG1/ABCG8. After uptake cholesterol is transported to plasma involving HDL and chylomicrons. HDL pathway was not affected, but chylomicron pathway was up regulated in *Clk*$^{\Delta 19/\Delta 19}$*Apoe*$^{-/-}$ mice. Two proteins, ACAT2 and MTP, involved in the assembly of chylomicrons were increased in *Clk*$^{\Delta 19/\Delta 19}$*Apoe*$^{-/-}$ mice. ACAT2 converts free cholesterol into cholesteryl esters and MTP transfers these cholesteryl esters to nascent lipoproteins to assist in the assembly and secretion of ApoB48-containing chylomicrons. Thus, Clock regulates cholesterol absorption by modulating cholesterol uptake, cholesterol esterification and chylomicron assembly.

This study shows that Clock$^{\Delta 19/\Delta 19}$ protein disrupts several macrophage functions; secretion of cytokines, uptake of oxidized lipoproteins and cholesterol efflux. *Clk*$^{\Delta 19/\Delta 19}$*Apoe*$^{-/-}$ macrophages secrete more IL12, IL17 and G-CSF. They take up more modified lipoproteins and retain higher amounts of oxidized lipids. Additionally, we showed that *Clk*$^{\Delta 19/\Delta 19}$*Apoe*$^{-/-}$ mice were defective in reverse cholesterol transport due to a combination of lower plasma cholesterol acceptors, ApoAI/HDL, and reduced macrophage expression of ABCA1 and ABCG1 transporters. Molecular studies revealed that Clock regulates ABCA1 and that USF2 might be an intermediary repressor that is regulated by Clock to modulate ABCA1 expression in macrophages. During Clock deficiency, USF2 levels are increased and there in enhanced association of this repressor with the ABCA1 promoter.

Consideration was given to the possibility that effects observed in *Clk*$^{\Delta 19/\Delta 19}$*Apoe*$^{-/-}$ mice might not be specific to Clock dysfunction. Instead, it could be a general effect due to deficiencies in other clock genes or due to off target effects of the mutation. To address this, we have performed several Clock knockdown experiments in WT macrophages. ABCA1 levels were reduced after siClock treatment. Further, there were no significant differences,

NIH-PA Author Manuscript

NIH-PA Author Manuscript

NIH-PA Author Manuscript

except for Per3 and Cry2 mRNA levels, in macrophages obtained from $Clk^{\Delta 19/\Delta 19}Apoe^{-/-}$ and $Apoe^{-/-}$ mice (Fig S11). Thus, Clock has a specific effect on lipid metabolism. It is known that Clock affects cholesterol synthesis and degradation by the liver. In our studies, we observed no significant increase in lipoprotein production by the liver. Therefore, we did not address whether hepatic cholesterol metabolism was affected in these mice.

Myocardial infarctions predominantly occur in the morning. It is known that circadian clocks regulate arrhythmogenesis, myocardial contractility and oxidative metabolism. Cheng et al. using an isograft model have shown that transplantation of arteries from Baml1 and Per deficient mice into wildtype mice elicits a pathologic response resulting in intimal hyperplasia and wall thickening [23]. This response was due to infiltration of wildtype cells and hyperplastic response by the clock-deficient arteries. Here, we provide evidence that Clock deficiency alters lipid metabolism and macrophage function to enhance atherosclerosis. Thus, circadian Clock might play an important protective role against hyperlipidemia and atherosclerosis.

In short, these studies show that Clock regulates cholesterol metabolism in the intestine and macrophages and acts as an anti-atherogenic gene (Fig S12). In the intestine, Clock deficiency increases lipid absorption. In macrophages, it augments uptake of modified lipoproteins and diminishes cholesterol efflux. These changes could contribute to enhanced atherosclerosis in $Clk^{\Delta 19/\Delta 19}Apoe^{-/-}$ mice.

Supplementary Material

Refer to Web version on PubMed Central for supplementary material.

Acknowledgments

We are grateful to Drs. Lita Freeman and Alan Remaley of the National Institutes of Health for plasmids expressing luciferase under the control of various ABCA1 promoter regions; Drs. Roman Kondratov and Antoch Marino for plasmids expressing Clock; Yan Li and Joyce Queiroz for technical assistance in the early analysis of atherosclerotic plaques; and Wei Quan for technical assistance in fluorescence microscope.

Funding Sources: This work was supported in part by the National Institutes of Health grant DK-81879 to MMH and the American heart Association Scientist Development Grant (2300158) to XP.

References

1. Bass J, Takahashi JS. Circadian integration of metabolism and energetics. Science. 2010; 330:1349–54. [PubMed: 21127246]
2. Hussain MM, Pan X. Clock genes, intestinal transport and plasma lipid homeostasis. Trends Endocrinol Metab. 2009; 20:177–85. [PubMed: 19349191]
3. DeBruyne JP, Noton E, Lambert CM, Maywood ES, Weaver DR, Reppert SM. A clock shock: mouse CLOCK is not required for circadian oscillator function. Neuron. 2006; 50:465–77. [PubMed: 16675400]
4. DeBruyne JP, Weaver DR, Reppert SM. CLOCK and NPAS2 have overlapping roles in the suprachiasmatic circadian clock. Nat Neurosci. 2007; 10:543–5. [PubMed: 17417633]
5. King DP, Zhao Y, Sangoram AM, Wilsbacher LD, Tanaka M, Antoch MP, Steeves TD, Vitaterna MH, Kornhauser JM, Lowrey PL, Turek FW, Takahashi JS. Positional cloning of the mouse circadian clock gene. Cell. 1997; 89:641–53. [PubMed: 9160755]
6. Vitaterna MH, King DP, Chang AM, Kornhauser JM, Lowrey PL, McDonald JD, Dove WF, Pinto LH, Turek FW, Takahashi JS. Mutagenesis and mapping of a mouse gene, Clock, essential for circadian behavior. Science. 1994; 264:719–25. [PubMed: 8171325]

NIH-PA Author Manuscript

NIH-PA Author Manuscript

NIH-PA Author Manuscript

7. Turek FW, Joshu C, Kohsaka A, Lin E, Ivanova G, McDearmon E, Laposky A, Losee-Olson S, Easton A, Jensen DR, Eckel RH, Takahashi JS, Bass J. Obesity and metabolic syndrome in circadian Clock mutant mice. Science. 2005; 308:1043–5. [PubMed: 15845877]
8. Pan X, Zhang Y, Wang L, Hussain MM. Diurnal regulation of MTP and plasma triglyceride by CLOCK is mediated by SHP. Cell Metab. 2010; 12:174–86. [PubMed: 20674862]
9. Pan X, Hussain MM. Clock is important for food and circadian regulation of macronutrient absorption in mice. J Lipid Res. 2009; 50:1800–13. [PubMed: 19387090]
10. Liu J, Huan C, Chakraborty M, Zhang H, Lu D, Kuo MS, Cao G, Jiang XC. Macrophage sphingomyelin synthase 2 deficiency decreases atherosclerosis in mice. Circ Res. 2009; 105:295–303. [PubMed: 19590047]
11. Pan X, Hussain MM. Diurnal regulation of microsomal triglyceride transfer protein and plasma lipid levels. J Biol Chem. 2007; 282:24707–19. [PubMed: 17575276]
12. Luchoomun J, Hussain MM. Assembly and secretion of chylomicrons by differentiated Caco-2 cells: Nascent triglycerides and preformed phospholipids are preferentially used for lipoprotein assembly. J Biol Chem. 1999; 274:19565–72. [PubMed: 10391890]
13. Iqbal J, Queiroz J, Li Y, Jiang XC, Ron D, Hussain MM. Increased intestinal lipid absorption caused by Ire1b deficiency contributes to hyperlipidemia and atherosclerosis in apolipoprotein E-deficient mice. Circ Res. 2012; 110:1575–84. [PubMed: 22556338]
14. Wang X, Collins HL, Ranalletta M, Fuki IV, Billheimer JT, Rothblat GH, Tall AR, Rader DJ. Macrophage ABCA1 and ABCG1, but not SR-BI, promote macrophage reverse cholesterol transport in vivo. J Clin Invest. 2007; 117:2216–24. [PubMed: 17657311]
15. Paigen B, Morrow A, Holmes PA, Mitchell D, Williams RA. Quantitative assessment of atherosclerotic lesions in mice. Atherosclerosis. 1987; 68:231–40. [PubMed: 3426656]
16. Fazio S, Linton MF. Mouse models of hyperlipidemia and atherosclerosis. Front Biosci. 2001; 6:D515–D525. [PubMed: 11229870]
17. Iqbal J, Hussain MM. Intestinal lipid absorption. Am J Physiol Endocrinol Metab. 2009; 296:E1183–E1194. [PubMed: 19158321]
18. Iqbal J, Anwar K, Hussain MM. Multiple, independently regulated pathways of cholesterol transport across the intestinal epithelial cells. J Biol Chem. 2003; 278:31610–20. [PubMed: 12775725]
19. Chen Z, O'Shea JJ. Regulation of IL-17 production in human lymphocytes. Cytokine. 2008; 41:71–8. [PubMed: 17981475]
20. Yang XP, Freeman LA, Knapper CL, Amar MJ, Remaley A, Brewer HB Jr. Santamarina-Fojo S. The E-box motif in the proximal ABCA1 promoter mediates transcriptional repression of the ABCA1 gene. J Lipid Res. 2002; 43:297–306. [PubMed: 11861672]
21. Schmitz G, Langmann T. Transcriptional regulatory networks in lipid metabolism control ABCA1 expression. Biochim Biophys Acta. 2005; 1735:1–19. [PubMed: 15922656]
22. Santamarina-Fojo S, Peterson K, Knapper C, Qiu Y, Freeman L, Cheng JF, Osorio J, Remaley A, Yang XP, Haudenschild C, Prades C, Chimini G, Blackmon E, Francois T, Duverger N, Rubin EM, Rosier M, Denefle P, Fredrickson DS, Brewer HB Jr. Complete genomic sequence of the human ABCA1 gene: analysis of the human and mouse ATP-binding cassette A promoter. Proc Natl Acad Sci U S A. 2000; 97:7987–92. [PubMed: 10884428]
23. Cheng B, Anea CB, Yao L, Chen F, Patel V, Merloiu A, Pati P, Caldwell RW, Fulton DJ, Rudic RD. Tissue-intrinsic dysfunction of circadian clock confers transplant arteriosclerosis. Proc Natl Acad Sci U S A. 2011; 108:17147–52. [PubMed: 21969583]

NIH-PA Author Manuscript
NIH-PA Author Manuscript
NIH-PA Author Manuscript

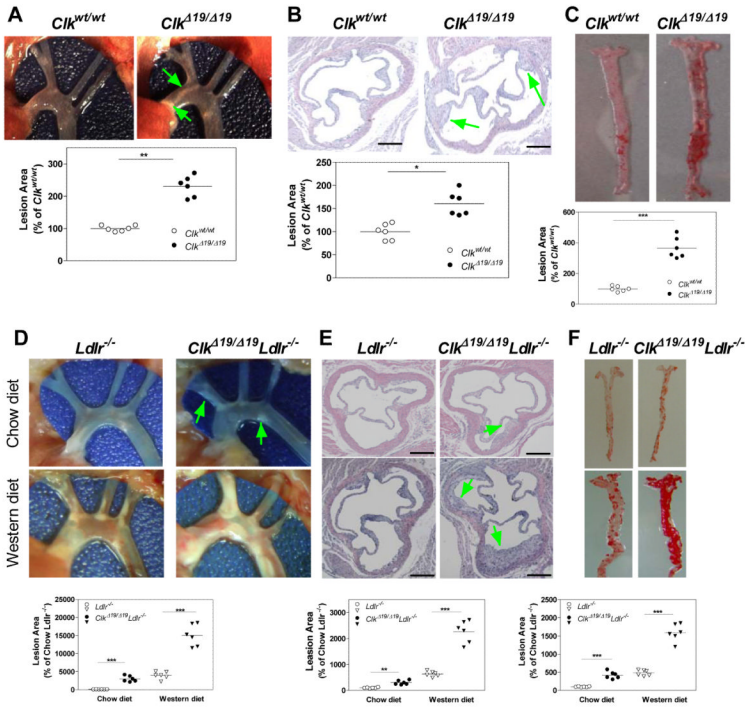

Figure 1.

Atherosclerosis in $Clk^{\Delta 19/\Delta 19}$ and $Clk^{\Delta 19/\Delta 19}Ldlr^{-/-}$ mice. **(A-C)** Male (8-12 weeks old) $Clk^{\Delta 19/\Delta 19}$ and $Clk^{wt/wt}$ littermates were fed an atherogenic diet for 2 months. Aortic arch was dissected and photographed; lesion areas were quantified using Image-Pro (A). Serial sections of cardiac/aortic junctions were stained with hematoxylin and eosin followed by lipid staining. Scale: 400 μm (B). Aortas were dissected and stained with Oil Red O and quantified (C). Mean±SD, n=6-9. * $P < 0.05$, ** $P < 0.01$, *** $P < 0.001$ compared to $Clk^{wt/wt}$ mice. **(D-F)** Male (8-12 weeks old) $Clk^{\Delta 19/\Delta 19}Ldlr^{-/-}$ and $Ldlr^{-/-}$ mice were fed a western or chow diet for 2 months. Aortic arches were dissected, photographed, and quantified (D). Sections from cardiac/aortic junctions were stained with hematoxylin and eosin followed by Oil Red O staining (E). Whole aortas were stained with Oil Red O and quantified (F). Mean±SD, n=9-12, ** $P < 0.01$, *** $P < 0.001$ compared to $Ldlr^{-/-}$ mice.

NIH-PA Author Manuscript

NIH-PA Author Manuscript

NIH-PA Author Manuscript

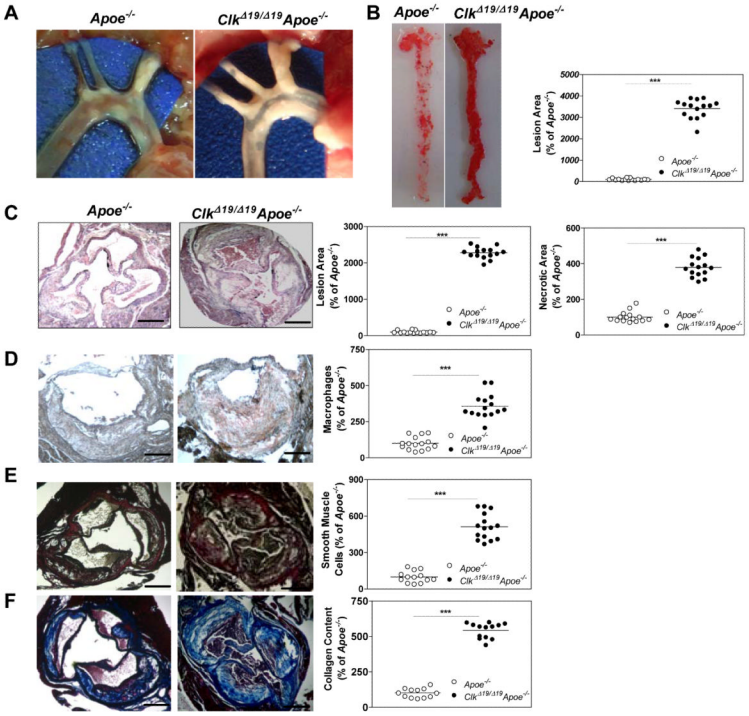

Figure 2.

Atherosclerosis in *Clk*$^{\Delta 19/\Delta 19}$*Apoe*$^{-/-}$ mice. **(A-B)** Chow fed, 8 month old, male, *Clk*$^{\Delta 19/\Delta 19}$*Apoe*$^{-/-}$ and *Apoe*$^{-/-}$ mice were dissected to visualize atherosclerotic lesions at the aortic arch (A). Whole aortas were stained with Oil Red O and lesions were quantified (B). **(C)** Sections from cardiac/aortic junctions were stained with hematoxylin and eosin followed by Oil Red O staining; lipid lesions and necrotic areas were quantified, Scale: 50 μm. **(D)** Sections were stained with anti-macrophage antibodies and quantified. (**E**) Sections were stained with β-actin to detect smooth muscle cells and were quantified, Scale: 400 μm. (**F**) Sections were stained with Masson Trichrome Collagen Staining kits and quantified. Mean±SD, n=12-15. * $P < 0.05$, ** $P < 0.01$, ***$P < 0.001$, compared to *Apoe*$^{-/-}$ mice, Scale: 400 μm.

NIH-PA Author Manuscript

NIH-PA Author Manuscript

NIH-PA Author Manuscript

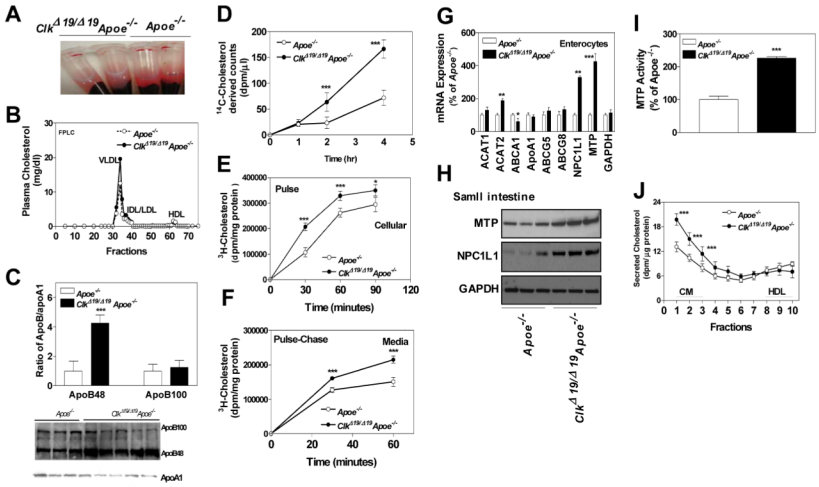

Figure 3.

Plasma lipids and cholesterol absorption in *Clk*$^{\Delta 19/\Delta 19}$*Apoe*$^{-/-}$ mice. **(A)** Blood was centrifuged to separate plasma and tubes were photographed. **(B)** Plasma was separated by FPLC and cholesterol was measured in fractions. **(C)** Plasma (1 μl) was western blotted (representative of n=10) to measure ApoB100, ApoB48 and ApoAI (bottom). Bands were quantified and ApoB/ApoAI ratios were plotted (top). .**(D)** *Clk*$^{\Delta 19/\Delta 19}$*Apoe*$^{-/-}$ mice absorb more cholesterol. Male mice were gavaged with radiolabeled cholesterol and plasma was collected to measure radioactivity. **(E)** To study uptake, isolated primary enterocytes were incubated with radiolabeled cholesterol. At different times, cells were collected to measure radioactivity and protein. **(F)** To study lipid secretion, primary enterocytes were incubated with radiolabeled cholesterol for 1.5 h, washed and then incubated in fresh media. At indicated times media were collected to measure radioactivity. Panels D-F were analyzed by two-way ANOVA. **(G)** RNA were isolated from enterocytes to measure different transporters. **(H-I)** Proximal jejunal pieces were homogenized and 20 μg protein was used to detect MTP and NPC1L1, and GAPDH by western blotting (H) and MTP activity (I). **(J)** Enterocytes isolated from *Clk*$^{\Delta 19/\Delta 19}$*Apoe*$^{-/-}$ or *Apoe*$^{-/-}$ small intestine were labeled for 1 hour with 0.5 μCi/mL of [^{3}H]cholesterol, washed and incubated with fresh media containing 1.6 mmol/L oleic acid in taurocholate micelles for 2 h [12, 18]. Media was used to separate lipoproteins by density gradient ultracentrifugation and radioactivity was determined in all fractions. Fractions 1 to 3 represent chylomicrons (CM), and fractions 8 to 10 represent HDL. Mean±SD, n=10, * $P < 0.05$, ** $P < 0.01$, *** $P < 0.001$ compared to *Apoe*$^{-/-}$ mice.

NIH-PA Author Manuscript

NIH-PA Author Manuscript

NIH-PA Author Manuscript

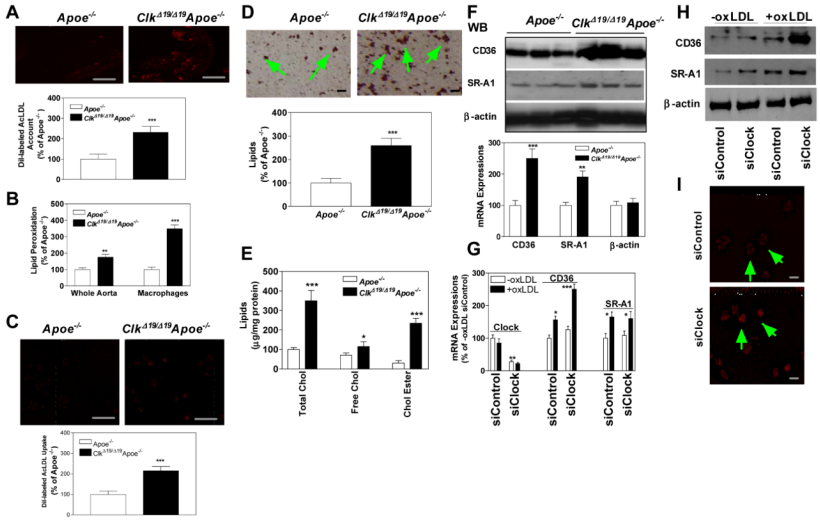

Figure 4.

Clk$^{\Delta 19/\Delta 19}$*Apoe*$^{-/-}$ macrophages take up more modified lipoproteins. **(A)** *Clk*$^{\Delta 19/\Delta 19}$*Apoe*$^{-/-}$ and *Apoe*$^{-/-}$ mice were injected with DiI-labeled Ac-LDL. After 18 h, sections from cardiac/aortic junctions were visualized under fluorescent microscope, photographed and quantified, Scale: 200 μm. **(B)** Lipid peroxides were measured in whole aorta or isolated macrophages as TBARS. **(C)** Wildtype bone marrow macrophages from C57Bl/6J mice were cultured for 7 days, incubated with DiI-labeled Ac-LDL for 6 h, visualized by fluorescent microscopy, photographed and quantified. Scale: 200 μm. **(D)** *Clk*$^{\Delta 19/\Delta 19}$*Apoe*$^{-/-}$ and *Apoe*$^{-/-}$ bone marrow macrophages were cultured for 7 days and stained with Oil Red O (top), Scale: 40 μm, and quantified by Image J (bottom). **(E)** Bone marrow macrophages were cultured for 7 days and used to measure total, free and esterified cholesterol. **(F)** Bone marrow macrophage were used to measure protein (n=3) and mRNA (n=6) levels of CD36 and SR-A1. Mean±SD, * $P < 0.05$, ** $P < 0.01$, *** $P < 0.001$ compared to *Apoe*$^{-/-}$ mice. **(G-H)** Wildtype bone marrow macrophages were treated with siControl or siClock. After 48 h, they were exposed to ox-LDL (200 μg/ml) or not for 6 h. RNA was isolated to quantify mRNA levels of Clock, CD36, or SR-A1 (G) or protein levels of CD36 and SR-A1 H). Mean± SD, n=9-10, * $P < 0.05$, ** $P < 0.01$, *** $P < 0.001$ compared to siControl cells not treated with oxLDL. **(I)** Wildtype bone marrow macrophages were treated with siControl or siClock. After 48 h, they were incubated with ox-LDL (200 μg/ml) and DiI-labeled AcLDL (5 μg/ml) for 6 h and visualized under a fluorescent microscope. Mean ± SD, n=9-10, * $P < 0.05$, compared to siControl, Scale: 20 μm.

NIH-PA Author Manuscript

NIH-PA Author Manuscript

NIH-PA Author Manuscript

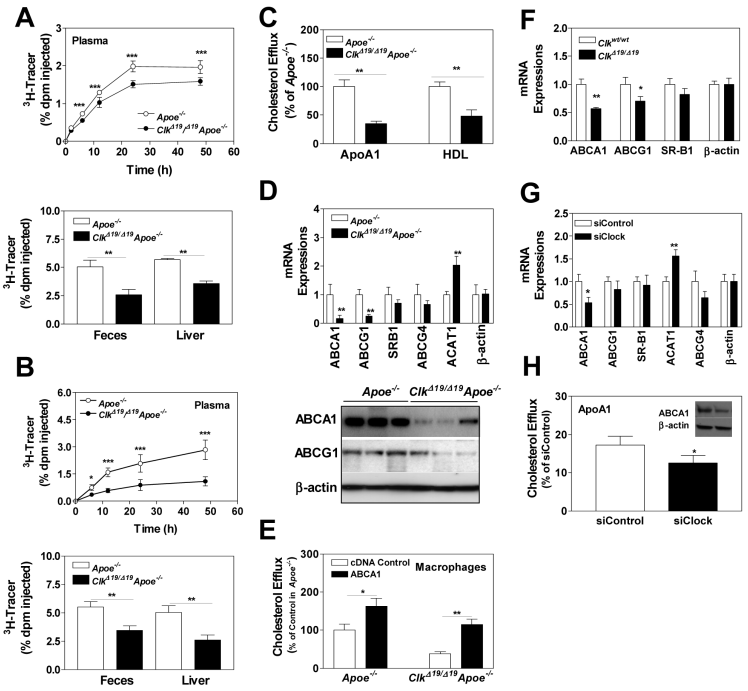

Figure 5.

Clk$^{\Delta 19/\Delta 19}$*Apoe*$^{-/-}$ macrophages are defective in reverse cholesterol transport. **(A)** J774A.1 macrophages were incubated with ^{3}H-cholesterol (5 μCi/mL) and AcLDL (50 μg/mL) for 24 h, and injected intraperitoneally into *Clk*$^{\Delta 19/\Delta 19}$*Apoe*$^{-/-}$ or *Apoe*$^{-/-}$ mice. At different times, plasma was obtained to measure counts. Feces was collected over 48 h, lipids were extracted and counted. At 48 h, liver segments were solubilized, counted, and normalized to liver weights. **(B)** *Clk*$^{\Delta 19/\Delta 19}$*Apoe*$^{-/-}$ or *Apoe*$^{-/-}$ macrophages were incubated with ^{3}H-cholesterol (5 μCi/mL) and AcLDL (50 μg/mL) for 24 h, and injected intraperitoneally into wildtype mice. At different times, plasma was used to measure counts. Feces was collected over 48 h, lipids were extracted and counted. At 48 h, liver segments were solubilized and counted. **(C)** *Clk*$^{\Delta 19/\Delta 19}$*Apoe*$^{-/-}$ or *Apoe*$^{-/-}$ macrophages were incubated with ^{3}H-cholesterol and AcLDL for 24 h, washed and incubated with purified ApoAI or HDL for 8 h. Cholesterol efflux is expressed as percent of cellular cholesterol. Values in *Apoe*$^{-/-}$ macrophages were normalized to 100%. **(D)** from *Clk*$^{\Delta 19/\Delta 19}$*Apoe*$^{-/-}$ and *Apoe*$^{-/-}$ macrophages were used to measure protein (bottom) and mRNA (top) levels of ABCA1, ABCG1, and mRNA levels of other transporters. **(E)** *Clk*$^{\Delta 19/\Delta 19}$*Apoe*$^{-/-}$ and *Apoe*$^{-/-}$ macrophages were transfected with a control plasmid or a plasmid expressing ABCA1 and used to measure cholesterol efflux to apoAI. **(F)** Macrophages from Clk$^{wt/wt}$ and Clk$^{\Delta 19/\Delta 19}$ siblings were used to measure mRNA levels of different transporters. **(G)** Wildtype macrophages were treated with siControl or siClock for 48 h and mRNA levels of different lipid transporters were quantified. **(H)** These macrophages were assessed for their ability to efflux cholesterol to purified ApoA1 (graph) and to measure protein levels of ABCA1 and β-actin (inset). Mean±SD, n=6-9, * $P < 0.05$, ** $P < 0.01$, *** $P < 0.001$.

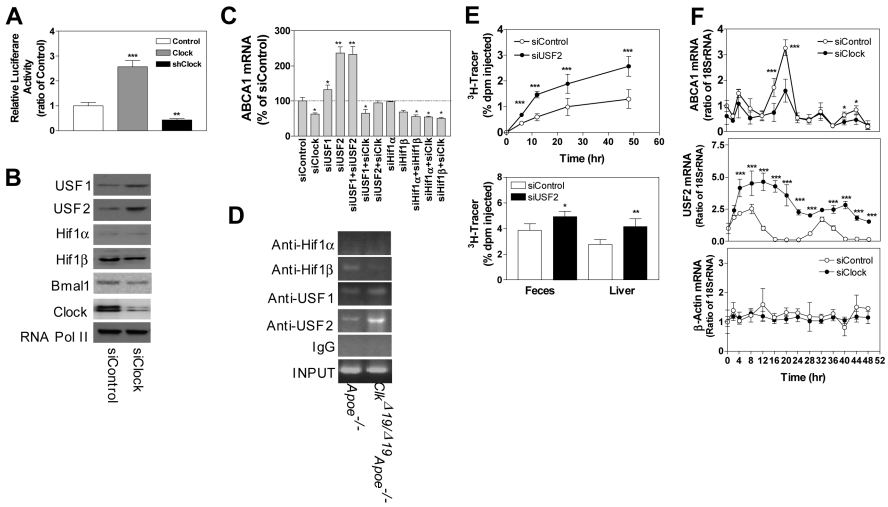

Figure 6.

Clock modulates expression of USF2 to regulate ABCA1. **(A)** Wildtype macrophages were transfected with a pGL3 plasmid expressing luciferase under the control of ABCA1 promoter along with a control plasmid, a plasmid expressing Clock or lentiviruses expressing shClock. After 72 h, cells were used to quantify luciferase activity. **(B)** Protein levels of different transcription factors were quantified in macrophages treated with siControl or siClock. **(C)** Wildtype macrophages were treated with different siRNAs, individually or in combination. After 48 h, mRNA levels of ABCA1 were quantified. **(D)** $Clk^{\Delta 19/\Delta 19}Apoe^{-/-}$ and $Apoe^{-/-}$ macrophages were cultured for 7 days. They were used to study the binding of different transcription factors to ABCA1 promoter by ChIP. Proteins were cross-linked to DNA, sheared and used to immunoprecipitate protein/DNA complexes using specific antibodies against indicated transcription factors. Sequences specific for ABCA1 promoter were amplified and separated on Agarose gels and visualized. **(E)** $Clk^{\Delta 19/\Delta 19}Apoe^{-/-}$ macrophages were treated with siControl or siUSF2 for 48 h, incubated with ^{3}H-cholesterol (5μCi/mL) and AcLDL (50 μg/mL) for 24 h, and injected intraperitoneally into wildtype mice. At different times, plasma was used to measure counts. Feces was collected over 48 h, lipids were extracted and counted. At 48 h, liver segments were solubilized and counted. **(F)** Wildtype bone marrow macrophages were treated with siControl or siClock for 48 h, incubated in serum-free media for 18 h, and for 2 h in media containing 50% fetal calf serum. Macrophages were washed and incubated in serum-free media. Three wells were harvested to measure ABCA1, USF2 as well as β-actin mRNA at indicated times. Comparisons were performed by two-way ANOVA. Mean±SD, n=6-9, * $P < 0.05$, ** $P < 0.01$, *** $P < 0.001$.

NIH-PA Author Manuscript NIH-PA Author Manuscript NIH-PA Author Manuscript

NIH-PA Author Manuscript
NIH-PA Author Manuscript
NIH-PA Author Manuscript

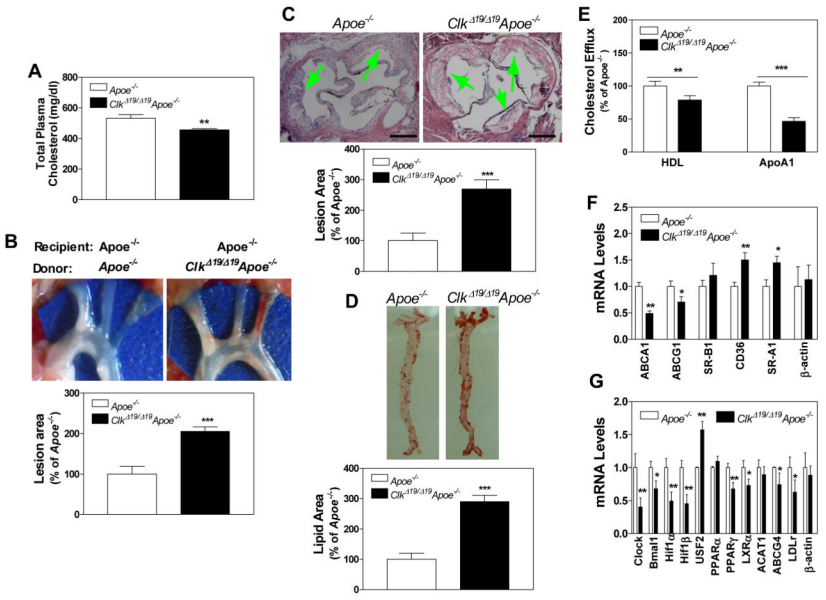

Figure 7.

Atherosclerosis in *Apoe*$^{-/-}$ mice transplanted with bone marrow cells derived from *Clk*$^{\Delta 19/\Delta 19}$*Apoe*$^{-/-}$ mice. Lethally irradiated *Apoe*$^{-/-}$ mice were transplanted with bone marrow cells obtained from *Clk*$^{\Delta 19/\Delta 19}$*Apoe*$^{-/-}$ or *Apoe*$^{-/-}$ mice. After 3 months, animals were started on a Western diet. Lesions and plasma lipids were quantified after 1 month. **(A)** Plasma was used to measure cholesterol. **(B)** Aortic arches were dissected, photographed, and lesions were quantified using Image-Pro. (**C**) Sections from cardiac/aortic junctions were stained with hematoxylin and eosin followed by Oil Red O staining and lipid lesions and necrotic areas were quantified, Scale: 500 μm. **(D) A**ortas were dissected, stained with Oil Red O, and quantified. (**E**) Bone marrow macrophages from *Apoe*$^{-/-}$ mice transplanted with *Clk*$^{\Delta 19/\Delta 19}$*Apoe*$^{-/-}$ or *Apoe*$^{-/-}$ bone marrow cells were incubated with ^{3}H-cholesterol and AcLDL for 18 h, washed and incubated with purified ApoAI or HDL for 8 h. Cholesterol efflux to media acceptors was expressed as percent of cellular cholesterol. **(F-G)** Bone marrow macrophages from irradiated *Apoe*$^{-/-}$ mice transplanted with *Clk*$^{\Delta 19/\Delta 19}$*Apoe*$^{-/-}$ and *Apoe*$^{-/-}$ bone marrow cells were used to measure mRNA levels of different lipid transporters (F) and transcription factors (G) that regulate ABCA1. Mean± SD, n=9-10, * $P < 0.05$, ** $P < 0.01$; *** $P < 0.001$ compared to control.

NIH-PA Author Manuscript
NIH-PA Author Manuscript
NIH-PA Author Manuscript

Table 1

Plasma lipid levels in different diet fed mice used in this study.

Lipid Metabolic Parameter	$Clk^{wt/wt}$ (n=9)	$Clk^{\Delta19/\Delta19}$ (n=9)	$Ldlr^{-/-}$ (n=9)	$Clk^{\Delta19/\Delta19}Ldlr^{-/-}$ (n=12)	$Apoe^{-/-}$ (n=12)	$Clk^{\Delta19/\Delta19}Apoe^{-/-}$ (n=12)
A. Chow Diet-fed						
Plasma Triglycerides (mg/dl)	90.1±14.7	150.2±10.9***	158.4 ± 8.7	280.6±22.9***	150.3±13.7	107.2±16.2**
Plasma Cholesterol (mg/dl)	80.6±10.5	155.1±12.0***	277.6±35.3	550.4±90.6**	546.4±45.0	1094.1±54.3**
Plasma Free Cholesterol (mg/dl)	20.3±6.0	36.2±4.11*	60.5±5.9	76.4±5.5**	36.1±5.3	68.7±8.2***
Plasma Cholesterol Ester (mg/dl)	60.8±5.7	119.0±10.5***	217.2±25.7	475.3±57.8**	510.3±56.3	1025.3±123.1***
Plasma Phospholipid (mg/dl)	172.2±10.8	200.2±17.2**	286.6±29.6	356.5±67.2	429.9±37.7	462.1±53.9
HDL-Cholesterol (mg/dl)	30.5±4.0	28.5±3.8	46.8±5.6	43.8±8.6	52.3±6.2	40.6±5.5*
ApoB-Lipoprotein Cholesterol (mg/dl)	50.4±5.2	125.0±6.1***	230.4±40.3	506.0±70.3**	504.2±52.5	1073.5±40.2**
Body weight (g)	26.3±2.3	30.9±2.7	30±2.5	33.5±2.4	30.5±2.0	33.6±2.1
B. Atherogenic diet fed						
Plasma Triglycerides (mg/dl)	56.2±7.2 #	129.7±6.6**,#				
Plasma Cholesterol (mg/dl)	293±25.8 ##	705.6±72.4***, ##				
Plasma free Cholesterol (mg/dl)	56±4.6 ###	75.8±7.9*, ##				
Plasma Cholesterol Ester (mg/dl)	236±40.6 ##	629.7±56.8***, ##				
Plasma Phospholipid (mg/dl)	150.3±12.5##	162.5±13.9 ##				
HDL-Cholesterol(mg/dl)	15.4±3.3 ###	14.3±2.7##				
ApoB-Lipoprotein Cholesterol (mg/dl)	267±30.4 ##	690.7±5.1***, ###				
Body weight (g)	19.56±2.8 #	19.30±3.7 ##				

NIH-PA Author Manuscript
NIH-PA Author Manuscript
NIH-PA Author Manuscript

Lipid Metabolic Parameter	**$Clk^{wt/wt}$ (n=9)**	**$Clk^{\Delta19/\Delta19}$ (n=9)**	**$Ldlr^{-/-}$ (n=9)**	**$Clk^{\Delta19/\Delta19}Ldlr^{-/-}$ (n=12)**	**$Apoe^{-/-}$ (n=12)**	**$Clk^{\Delta19/\Delta19}Apoe^{-/-}$ (n=12)**
C. Western diet fed						
Plasma Triglycerides (mg/dl)	-	-	450.2±56.1 ##	600.6±78.4 *, ##	56±5.364 ##	49.26±7.4 **,##
Plasma Cholesterol	-	-	650.4±90.6 ##	1290.2±80.5 ***,###	750.6±100.1 #	1356.4±120.5 ***,#
Plasma Free Cholesterol (mg/dl)	-	-	230.6±31.0 ##	350.8±67.2 *,#	98.8±14.2 ##	145.6±15.0 **, ##
Plasma Cholesterol Ester (mg/dl)	-	-	420.0±29.6 ###	940.0±79.1 **,###	652.0±50.1 ###	1210.3±119.3 ***
Plasma Phospholipid (mg/dl)	-	-	500.8±37.4 ###	608.6±59.1 ##	560.8±60.5 ##	660.1±70.5 #
HDL-Cholesterol (mg/dl)	-	-	70.9±5.0 ###	64.3±7.8 ###	35.7±3.0 #	29.3±4.7
ApoB-Lipoprotein Cholesterol (mg/dl)	-	-	580.1±80.2 ##	1226.0±90.1 ***,###	715.4±50.1 ###	1327.0±70.8 **, ##
Body weight (g)	-	-	33.5±3.8 #	35.6±2.9 #	35.5±2.0	37.80±3.2

Changes in lipid/metabolic parameters for different mutant mice were compared (left column to right column) with their control animals $Clk^{wt/wt}$, $Ldlr^{-/-}$, $Apoe^{-/-}$, respectively, and significant differences are designated as *P<0.05; ** P<0.01 and *** P<0.001, Mean ± SD.

Effect of feeding different diets was compared (top to bottom) with chow fed animals for each genotype. Significant differences are shown as # P<0.05; ## P<0.01 and ### P<0.001.